Including a Luminous Central Remnant in Radiative Transfer Simulations for Type Iax Supernovae

F. P. Callan[1], S. A. Sim[1], C. E. Collins[2], L. J. Shingles[3], F. Lach[4], F. K. Röpke[4,5], R. Pakmor[6] and S. Srivastav[7]

[1] Astrophysics Research Centre, Queen's University Belfast, BT7 1NN, United Kingdom, [2] School of Physics, Trinity College Dublin, The University of Dublin, Dublin 2, Ireland,
[3] GSI Helmholtzzentrum für Schwerionenforschung, Planckstraße 1, 64291 Darmstadt, Germany, [4] Heidelberger Institut für Theoretische Studien, Germany, [5] Zentrum für Astronomie der Universität Heidelberg, Germany,
[6] Max-Planck-Institut für Astrophysik, Karl-Schwarzschild-Str. 1, D-85748, Garching, Germany, [7] Astrophysics sub-Department, Department of Physics, University of Oxford, Keble Road, Oxford OX1 3RH, UK

Introduction

Type Iax supernovae (SNe Iax) are the most numerous peculiar sub-class of Type Ia supernovae (SNe Ia), estimated to make up ~15% of the total Ia rate (Srivastav et al. 2022). They have been proposed to arise from deflagrations of Chandrasekhar mass white dwarfs (WDs) as the properties of such explosions naturally reproduce many of the observed characteristics of SNe Iax such as their sub-luminous lightcurves (e.g. Jordan et al. 2012; Fink et al. 2014). Pure deflagration model sequences are also able to reproduce much of the substantial observed diversity in peak brightness of the SNe Iax class (Fink et al. 2014; Lach et al. 2022). However, the model light curves decline too quickly after peak, particularly for red optical and near infrared (NIR) bands (Kromer et al. 2013; Fink et al. 2014; Lach et al. 2022). Some deflagration models do not fully unbind the WD, leaving a remnant polluted with ^{56}Ni (e.g. Jordan et al. 2012; Fink et al. 2014) which could contribute to the optical display. Such a luminous remnant may have been detected in late time observations of SNe Iax (e.g. Foley et al. 2014; McCully et al. 2022).

Including a luminous remnant in radiative transfer simulations

We use the 3D, time-dependent, Monte-Carlo radiative transfer code ARTIS (Kromer & Sim 2009; Shingles et al. 2020), with the NLTE approximation described by Kromer & Sim (2009), to investigate the impact of including treatment for a luminous remnant in radiative transfer simulations of deflagration explosion models from the sequence of Lach et al. (2022) [hereafter L22]. This enables robust bolometric light curves to be calculated (see Fig. 1) as well as predictions of band lightcurves and spectra for models including the remnant contribution. The remnant ^{56}Ni masses adopted are informed by the predictions of the L22 hydrodynamic explosion simulations (see Table 1). The standard L22 deflagration models are denoted as rX_dY_Z (r is ignition spark offset, d the WD central density and Z metallicity relative to solar). We differentiate models including the remnant contribution with an "R" and include information on the remnant temperature in the model name, except for our model with fixed remnant radius and thus evolving temperature (denoted as "const rad").

Model	$M(^{56}\mathrm{Ni})_{\mathrm{rem}}$	T_{rem} (K)
r10_d4.0_Z_R_2000K	0.054 (1)	2000
r10_d4.0_Z_R_8000K	0.054 (1)	8000
r10_d4.0_Z_R_15000K	0.054 (1)	15000
r10_d4.0_Z_R_const_rad	0.054 (1)	-
r48_d5.0_Z_R_6000K_0.33Ni	0.013 ($\frac{1}{3}$)	6000
r114_d6.0_Z_R_4000K	0.030 (1)	4000
r114_d6.0_Z_R_6000K_0.1Ni	0.003 ($\frac{1}{10}$)	6000

Table 1: Adopted remnant ^{56}Ni masses in solar masses with the fraction of the remnant ^{56}Ni mass predicted by the L22 simulations that these represent included in brackets.

We make the following key assumptions about the remnant in our simulations:

- The remnant emits centrally.
- The remnant emits instantaneously according to the ^{56}Ni decay chain.
- Each decay results in the emission of a Monte Carlo photon packet drawn from a black body distribution with assumed characteristic temperature.
- Once emitted the Monte Carlo packets escaping from the remnant travel through the ejecta and can interact through all the same processes as packets originating in the ejecta.

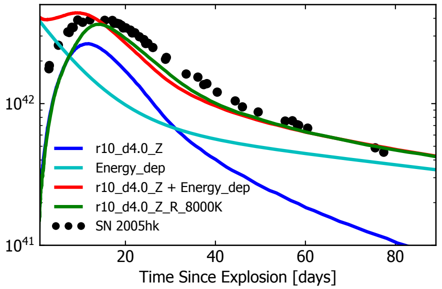

Fig. 1: Bolometric light curves for the r10_d4.0_Z L22 model and our new r10_d4.0_Z_R_8000K simulation. We also show the remnant ^{56}Ni energy deposition and the light curve obtained by adding this to the r10_d4.0_Z light curve (following the approach of Kromer et al. 2013). The bright SN Iax, 2005hk (Phillips et al. 2007) is included for comparison. While adding the remnant energy deposition to the standard deflagration model predicts a bolometric light curve which better matches the decline of SN 2005hk it is too bright before peak. Including treatment for the interaction of the remnant radiation with the ejecta is therefore required to accurately represent the bolometric lightcurves.

Comparisons with bright SNe Iax

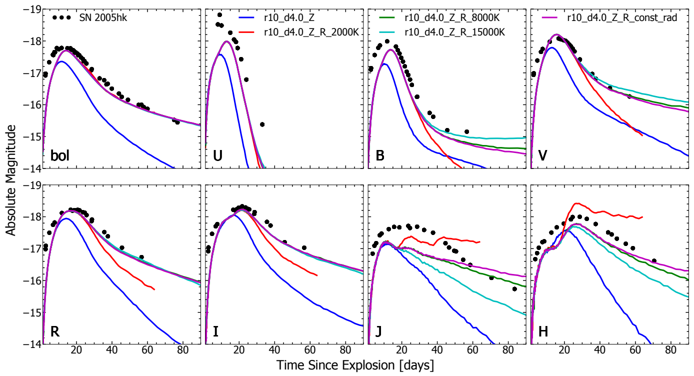

Fig 2: Angle averaged bolometric and *UBVRIJH*-band light curves for the r10_d4.0_Z L22 model and four new models in which we also treat energy injected by radioactive decays in a luminous remnant in our radiative transfer simulations. Included for comparison are light curves of SN 2005hk (Phillips et al. 2007), a bright SN Iax.

- Including treatment for the remnant energy injection significant improvement agreement with the bolometric and band light curves of bright SNe Iax such as SN 2005hk compared to the standard deflagration models (see Fig. 1 and 2).
- Our simulations are not overly sensitive to the choice of remnant temperature at a given time. Adopting fixed remnant temperatures of 8000 K and 15000 K or a remnant with fixed radius (and thus evolving temperature) produce similarly good agreement with SN 2005hk.
- The poor agreement with the band lightcurves of SN 2005hk rules out a remnant temperature of 2000 K for our models.

Comparisons with intermediate luminosity SNe Iax

- Including the remnant significantly improves agreement with the light curves of the intermediate luminosity SN 2019muj (see Fig. 3).
- Of the models investigated in this work, intermediate-luminosity deflagration models with remnant contribution included display the greatest improvement in agreement with observed SNe Iax relative to standard deflagration models.
- Our model which produces best agreement with SN 2019muj assumes a remnant ^{56}Ni mass only a third of that predicted by the L22 explosion simulation: including the entire remnant ^{56}Ni mass predicted for fainter deflagration models results in light curves with significantly too much NIR flux to provide a good match to SN 2019muj (see model r114_d6.0_Z_R_4000K in Fig. 3).

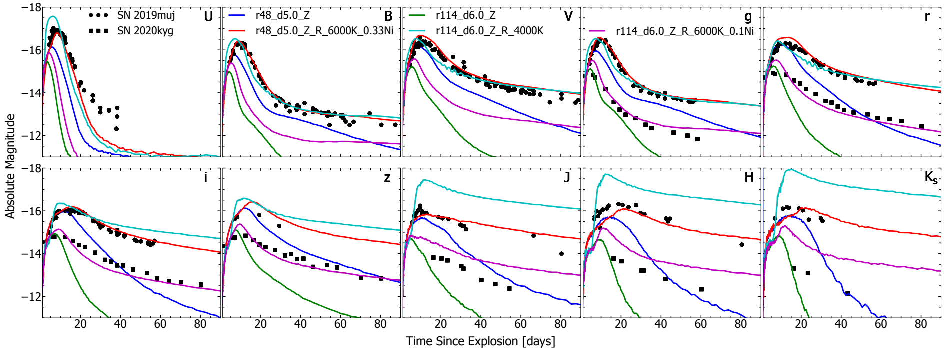

Fig 3: Angle averaged *UBVJHKs* and *griz*-band light curves for the r48_d5.0_Z_R_6000K_0.33Ni, r114_d6.0_Z_R_4000K and r114_d6.0_Z_R_6000K_0.1Ni models along with the L22 r48_d5.0_Z and r114_d6.0_Z models. The light curves of SN2019muj (Barna et al. 2021; Kawabata et al. 2021), an intermediate-luminosity SN Iax and the faint SN 2020kyg (Srivastav et al. 2022) are included for comparison.

Comparisons with faint SNe Iax

- Including treatment for the remnant significantly improves agreement with the light curves of the faint SN 2020kyg primarily due to the significantly slowed decline post peak in all bands (see Fig. 3).
- Our model in best agreement with SN 2022kyg assumes a remnant ^{56}Ni mass only a tenth of that predicted by the L22 explosion simulations.
- Including this remnant contribution still results in light curves that are too bright at peak in all bands relative to SN 2020kyg and particularly in NIR bands.

Implications for the remnant

Our models in best agreement with intermediate-luminosity and faint SNe Iax adopt remnant ^{56}Ni masses a third and a tenth of those predicted by the L22 explosion simulations (see Table 1). This suggests not all the energy injected in the remnant can contribute to the optical display. Potentially explanations for this include:

- A substantial fraction of the energy deposited in the remnant driving a wind in the remnant envelope as proposed by Shen & Schwab (2017).
- A substantial fraction of the energy injected in the remnant contributing to a secondary mass ejection in the remnant, as suggested by Maeda & Kawabata (2022).
- Diffusion timescales in the remnant are long enough that they lead to significant delays in the radiation contributing to the optical display (Maeda & Kawabata 2022).

Difficulty matching the faintest Iax

The faintest observed SN Iax is at least a magnitude fainter at peak than SN 2020kyg (Karambelkar et al. 2021). However, including only a tenth of the remnant ^{56}Ni mass predicted by the explosion simulation of the faintest deflagration model in the L22 sequence produces light curves that are already too bright relative to SN 2020kyg (model r114_d6.0_Z_6000K_0.1Ni in Fig 3.). Therefore, for deflagration models to achieve agreement with the faintest observed SNe Iax while including the remnant contribution they require an ejecta component more than a magnitude fainter than the faintest L22 model.

Future work

Including the energy injected from a luminous remnant in our radiative transfer simulations leads to significantly improved agreement with observations, strengthening the case of pure deflagration models for SNe Iax. However, outstanding questions remain. Future work should therefore:

- Explore the importance of NLTE effects and in particular investigate if the remnant is required to explain the peculiar late time spectra of observed SNe Iax as suggested by Foley et al. (2016).
- Follow the remnant more closely with hydrodynamical simulations to provide detailed remnant structures and insight into its likely evolution and emission.
- Further investigate the possibility of radioactively driven winds and delayed radioactive decays suggested by Shen & Schwab (2017) and the secondary remnant mass ejection proposed by Maeda & Kawabata (2022).
- Carry out hydrodynamic explosion simulations exploring whether even fainter pure deflagration models that could match the very faintest SNe Iax can be produced.

References

Barna, et al., 2021, MNRAS, 501, 1078
Fink et al., 2014, MNRAS, 438, 1762
Foley et al., 2014, ApJ, 792, 29
Foley et al., 2016, MNRAS, 461, 433
Jordan et al., 2012, ApJ, 761, L23
Karambelkar et al., 2021, ApJ, 921, L6
Kawabata et al., 2021, PASJ, 73, 1295
Kromer & Sim, 2009, MNRAS, 398, 1809
Kromer et al., 2013, MNRAS, 398, 1809
Lach et al., 2022, A&A, 658, A179
Maeda & Kawabata, 2022, ApJ, 941, 15
McCully et al., 2022, ApJ, 925, 138
Phillips et al., 2007, PASP, 119, 360
Shingles et al., 2020, MNRAS, 492, 2029
Srivastav et al., 2022, MNRAS, 511, 2708
Shen & Schwab, 2017, ApJ, 834, 180

Acknowledgements

The work presented here has made use of the HPC facilities of DiRAC, UK and Juelich, Germany.

QUEEN'S UNIVERSITY BELFAST

See paper here for details, or come talk to me :)

Contact details

f.callan@qub.ac.uk